DE GRUYTER

Chemical Papers 69 (1) 192–201 (2015)
DOI: 10.2478/s11696-014-0590-2

ORIGINAL PAPER

Synthesis of carbon quantum dots for DNA labeling and its electrochemical, fluorescent and electrophoretic characterization

[a]Vedran Milosavljevic, [a]Hoai Viet Nguyen, [a]Petr Michalek, [b]Amitava Moulick, [a,b]Pavel Kopel, [a,b]Rene Kizek, [a,b]Vojtech Adam*

[a] *Department of Chemistry and Biochemistry, Faculty of Agronomy, Mendel University in Brno, Zemedelska 1, CZ-613 00 Brno, Czech Republic*

[b] *Central European Institute of Technology, Brno University of Technology, Technicka 3058/10, CZ-616 00 Brno, Czech Republic*

Received 27 January 2014; Revised 17 March 2014; Accepted 18 March 2014

Nanoparticles as a progressively developing branch offer a tool for studying the interaction of carbon quantum dots (CQDs) with DNA. In this study, fluorescent CQDs were synthesized using citric acid covered with polyethylene glycol (PEG) as the source of carbon precursors. Furthermore, interactions between CQDs and DNA (double-stranded DNA and single-stranded DNA) were investigated by spectral methods, gel electrophoresis, and electrochemical analysis. Primarily, the fluorescent behavior of CQDs in the presence of DNA was monitored and major differences in the interaction of CQDs with tested single-stranded DNA (ssDNA) and double-stranded DNA (dsDNA) were observed at different amounts of CQDs (μg mL^{-1}: 25, 50, 100, 250, 500). It was found that the interaction of ssDNA with CQDs had no significant influence on the CQDs fluorescence intensity measured at the excitation wavelengths of 280 nm, 350 nm, and 400 nm. However, in the presence of dsDNA, the fluorescence intensity of CQDs was significantly increased. Our results provide basic understanding of the interaction between CQDs and DNA. Such fabricated CQDs–DNA might be of great benefit for the emerging nanomaterials based biosensing methods.

Keywords: carbon quantum dots, DNA, spectrophotometry, gel electrophoresis, electrochemical analysis

Introduction

The unique quantum size effect of quantum dots (QDs) semiconductor nanocrystal stems from dimensions smaller than the bulk exaction Bohr radius. This unique effect is connected with QDs properties such us broad excitation spectrum, excellent photostability, high quantum yield of fluorescence and high photobleaching (Song et al., 2013; Yang et al., 2013). The main advantage of semiconductor nanocrystals is their high fluorescence, where organic fluorophores usually do not have the excellent characteristics of QDs that are associated with their high photostability and resistance to photobleaching. Moreover, the spectral properties as emission and excitation can be changed easily based on the change of the size of semiconductor nanocrystals (Fu et al., 2005). On the other hand, an application of these semiconductor based QDs such as CdTe, CdSe, CdSe/ZnSe, PbS, and CdS (Ryvolova et al., 2012; Pohanka, 2014) is limited by the presence of heavy metals. This serious problem can be, however, overcome due to the extremely low concentration needed for their practical applications (Liu et al., 2011; Song et al., 2013). Compared with these semiconductor nanomaterials, CQDs show many advantages including chemical stability, biocompatibility and low toxicity (Bai et al., 2011; Dong et al., 2010).

CDQs represent a new type of nanomaterials with

*Corresponding author, e-mail: vojtech.adam@mendelu.cz

nanocrystal structure where the crystal size is not generally lower than 10 nm in diameter. The importance of CQDs is reflected in their electronic, mechanical, chemical and optical properties. All of these properties allow using CQDs in different fields of research such as catalysis, sensing, bioimaging, tissue engineering, optoelectronic and electronic devices (Bai et al., 2011; Dong et al., 2013; Yang et al., 2013; Zhang et al., 2013). Carbon nanoparticles have functionalized and passivated surface states with carboxyl or hydroxyl groups with good photo-induced electron transfer properties (Li et al., 2013a). There are many different ways to synthesize various functionalized and nonfunctionalized CQDs. These properties depend on the different methods of CQDs preparation such as pyrolysis (Jia et al., 2012), electrochemical exfoliation (Li et al., 2011a; Long et al., 2012; Ming et al., 2012), acidic oxidation (Liu et al., 2012), hydrothermal treatments (Sahu et al., 2012), microwave passivation (Li et al., 2011b), laser ablation (Cao et al., 2007), thermal oxidation, and emulsion-assisted methods (Bourlinos et al., 2008; Linehan & Doyle, 2014). Previously mentioned methods allow fast synthesis of CQDs with very high quality using low cost raw materials (Kwon et al., 2013; Liang et al., 2013; Liu et al., 2011). Materials for the preparation of CQDs depend on the methods used. Commonly used are carbon materials with different sizes such as graphite, carbon nanotubes, carbon soot, activated carbon, graphite oxide or different molecular precursors such as citric acid or glucose (Dong et al., 2012a). Excellent optical properties of CQDs originate from carboxyl or hydroxyl groups passivated by a polymer. These ensure the production of high fluorescent nanomaterials with high quantum yield and excitation wavelength (Kim et al., 2013). In addition, the unique photophysical and chemical properties of CQDs have attracted special attention for their potential application in biosensing (Dong et al., 2012b).

Biological macromolecules, such as DNA, can specifically interact with organic compounds (Zhao et al., 2014) which show certain limitations associated with long term photostability and solubility. For biological applications it is necessary to use water soluble materials with excellent photostability and optical properties. Semiconductor quantum dots characteristics allow using these properties for the production of new biosensors, which leads to their implementation in bio-analytical applications. These biosensors enable the detection and diagnosis of different types of illness and disease (Vaishnavi & Renganathan, 2014). Because of its natural molecular recognition and structure properties, DNA represents a suitable biomaterial for the interaction with other nanomaterials (He et al., 2011). Many various prototypes of biosensors were prepared by QDs–DNA conjugation using the advantage of the excellent properties of QDs and the flexibility and precision of interparticle distance tuning by the DNA strand; moreover, this method represents the easiest way of assembling heterogeneous nanostructures via the DNA mediated approach (Grimes et al., 2006; Wang et al., 2011). CQDs are also considered as materials with great potential to be used for DNA analysis (Pandey et al., 2014; Su et al., 2014).

In the present article, the preparation of CQDs covered with polyethylene glycol by a simple hydrothermal approach and the interaction of the prepared CQDs with DNA are presented. The effect of the DNA conjugation process on the structural stability of a polymer on a particular surface of CQDs and on the stability of CQDs, as well on the interaction between CQDs and DNA was the main aim of this research. The effect of the CQDs conjugation with DNA and the effect of this conjugation on the CQDs stability were investigated. Also a part of the experiments was done to investigate the effect of the initial CQDs/DNA ratio on the amount of CQDs per ssDNA and dsDNA. According to the results obtained, the difference between the fluorescence of the CQDs sample and CQDs–ssDNA was very small; however, in case of the CQDs–dsDNA sample, the fluorescence intensity increase was much higher than in case of CQDs or CQDS–ssDNA samples, which enables to distinguish ssDNA and dsDNA. This shows that methods employing CQDs–dsDNA provide a significant benefit in DNA labeling. Spectral methods, electrochemical analysis, and gel electrophoresis were employed to investigate the interaction between CQDs and DNA.

Experimental

Chemicals and materials

Citric acid, polyethylene glycol (PEG) with molecular mass of 8000, ethylene glycol, sequence of the forward primer 5′-CGCAAGAGAGGGATCAACTT-3′, reverse primer 5′-TATTTCAATGCCTCGGCTCT-3′, ACS H_2O, tris-hydroxymethyl-aminomethane, acetic acid, ethylenediaminetetraacetic acid, and ethidium bromide were purchased from Sigma–Aldrich Co. (St. Louis, MO, USA). A D-TUBE Dialyzer maxi MWCO 3.5 kDa was purchased from EMD Milipore Corporation (San Diego, CA, USA). Deionized water underwent demineralization by reverse osmosis using an Aqua Osmotic 02 (Aqua Osmotic, Czech Republic) and was subsequently purified using a Millipore RG (MiliQ water, 18 M, Millipore Corp., Billerica, MA, USA). Universal soft tin containers were purchased from Thermo-Fisher Scientific (Cambridge, UK). The Transcriptor First Strand cDNA Synthesis Kit and the MagNA Pure Compact RNA Isolation Kit were purchased from Roche (Basel, Switzerland). The *Taq* PCR kit was bought from New England BioLabs (Ipswich, MA, USA). Agarose was purchased from AppliChem (Darmstadt, Germany). RNA-later solution was purchased from Ambion (Austin, TX, USA).

Synthesis of CQDs

Common methods for the preparation of water soluble CQDs were adopted according to Wang et al. (2010a). Briefly, the solution of ethylene glycol (10 mL), PEG-8000 (1 g) and citric acid (1 g) in a 100 mL three-neck flask was heated at 180 ℃ for 3 h under nitrogen flow, and then cooled down to ambient temperature. Mili-Q water was then added and the mixture was stirred for a couple of minutes. The obtained solutions were purified for 24 h by dialysis against Mili-Q water with a D-Tube maxi dialyzer to remove ethylene glycol. Measurements of CQDs fluorescence were conducted by a multifunctional microplate reader Tecan Infinite 200 PRO (Tecan group Ltd., Männedorf, Switzerland). The absorbance scans were recorded in the range of 200–800 nm each 5 nm. Emission wavelengths were measured at different excitation wavelengths (280 nm, 350 nm, and 400 nm) with 2 μL of the sample placed on a NanoQuant plate, 16 well, with a quartz optical lens. The CQDs freeze-drying procedure was conducted using a Christ Alpha 1-2 (B. Braun Biotech International, Basel, Switzerland). C, H, N, and S content analysis was performed using a CHNS organic elemental analyzer Flash 2000 (Thermo-Fisher Scientific Inc., Waltham, MA, USA). Dried sample of CQDs was added into soft tin containers and burned at 950 ℃.

Metallothionein–DNA amplification and agarose gel electrophoresis

Amplification of DNA and preparation of polymerase chain reaction (PCR) products was conducted as follows: Isolation process was set according to the manufacturer's instructions using a MagNA Pure Compact (Roche, Basel, Switzerland). The mRNA obtained from earthworms was converted to cDNA employing a Transcriptor First Strand cDNA Synthesis Kit according to the manufacturer's instructions using the random hexamer primer. PCR tubes with the mixture were placed into a cycler reactor Mastercyclerc ep realplex 4S (Eppendorf AG, Hamburg, Germany) for cycling as follows: incubation at 25 ℃ for 10 min, followed by incubation at 55 ℃ for 30 min, inactivation of transcriptor reverse transcriptase by heating to 85 ℃ for 5 min and termination of the reaction by placing the tube on ice. cDNA was amplified using the *Taq* kit. The sequence of the forward primer was 5′-CGCAAGAGAGGGATCAACTT-3′ and the sequence of the reverse primer was 5′-TATTTCAATG CCTCGGCTCT-3′. The reaction mixture (25 μL) was composed of 10 × standard Taq reaction buffer (2.5 μL), 10 mM deoxynucleotide solution mix (0.5 μL), 1 μL of each primer (10 μM), 5 U μL^{-1} Taq DNA polymerase (0.2 μL), ACS purity sterile H_2O (17.3 μL), and cDNA (2.5 μL) obtained in the previous step. From this sample, the 228-bp PCR product of the metallothionein gene was obtained. The PCR product was mixed with CQDs and run in a 2 % agarose gel electrophoresis using agarose in 1 × TAE buffer (containing 40 mM trishydroxymethyl-aminomethane, 20 mM acetic acid, and 1 mM ethylenediaminetetraacetic acid) for 0 min, 5 min, 10 min, 15 min, 20 min, 25 min, 30 min, and 45 min at 60 V, respectively, using the electrophoretic apparatus. The bands were visualized by a UV transilluminator (VilberLourmat, Marne-la-Vallée Cedex, France) at 312 nm. Ethidium bromide was used to stain the PCR product. Measurements of PCR fluorescence were conducted by a multifunctional microplate reader Tecan Infinite 200 PRO. The absorbance scans were recorded in the range of 200–800 nm each 5 nm. Emission wavelengths were measured at different excitation wavelengths (280 nm, 350 nm, and 400 nm) with 2 μL of the sample placed on a NanoQuant plate, 16 well, with a quartz optical lens.

AdT SWV determination of CA peak from DNA–CQDs complex

Electrochemical measurements were performed on an AUTOLAB Analyzer (EcoChemie, Utrecht, Netherlands) connected to a VA-Stand 663 (Metrohm, Herisau, Switzerland) using a standard cell with three electrodes. A hanging mercury drop electrode (HMDE) with the drop area of 0.4 mm^2 was employed as the working electrode. An Ag/AgCl/3 M KCl electrode served as the reference electrode and a glassy carbon electrode was used as the auxiliary electrode. Software GPES 4.9 supplied by EcoChemie was employed for smoothing and baseline correction. All measurements were performed in the presence of the acetate buffer (0.2 M CH_3COOH and 0.2 M CH_3COONa, pH 5.0) at 25 ℃. Double-stranded DNA (dsDNA) and single-stranded DNA (ssDNA) were applied to interact with CQDs on the surface of the working electrode. Square wave voltammetry coupled with the adsorptive transfer technique (AdT SWV) was employed in this study. Conditions of the electrochemical determination were as follows: purge time: 120 s; frequency: 280 Hz; initial potential: 0 V; end potential: –1.8 V; potential step: 0.005 V; amplitude: 0.025 V. pH value was measured using the inoLab Level 3 (Wissenschaftlich-Technische Werkstatten GmbH, Weilheim, Germany).

Results and discussion

Effect of CQDs on DNA interactions

In this part, fluorescent CQDs were synthesized and the possibility of their interaction with DNA was examined using citric acid covered with PEG as the source of carbon precursors and live earthworms as the source of DNA. Covering of the CQD surface and

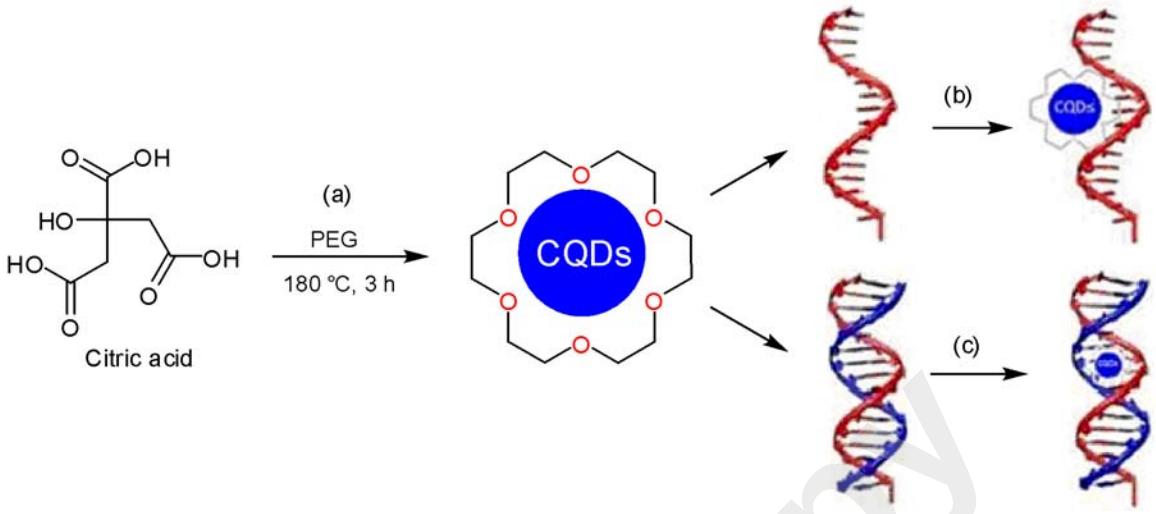

Fig. 1. Synthesis of PEG-functionalized CQDs (using citric acid as the carbon source and PEG as the capping agent) (a) and its interaction with: ssDNA (10 μg mL^{-1}) (b) and dsDNA (10 μg mL^{-1}) (c) using different amounts of CQDs (μg mL^{-1}: 25, 50, 100, 250, 500), measured immediately after mixing.

its interaction with single- and double-stranded DNA is shown in Fig. 1.

Water soluble CQDs were prepared according to the general method reported by Wang et al. (2010a). Heating of the solution helped to carbonize the molecular precursor. To produce CQDs, high temperature (180 ℃) is needed and nitrogen atmosphere was used here to reach the temperature required for the carbonization of the molecular precursor because the presence of oxygen during the heating process can lead to product oxidation. Higher temperature can cause the destruction of organic capping reagents which can result in bad surface passivation and functional group deprivation. Using citric acid as the carbon source, the loss of organic matter was prevented and the good properties of surface passivation were preserved. Low carbonization temperature (< 180 ℃) of citric acid enabled the synthesis of functionalized CQDs. To achieve nanomaterial stability, surface capping agent PEG was used. The polymer provided surface functionality, which leads to the enhanced luminescence and chemical stability as confirmed by fluorescence intensity measurements showing that after two months, CQDs have high luminescence and bright blue color. Chemical composition of CQDs was confirmed by elemental analysis. A sample for CHNS analysis was prepared in these steps: CQDs sample (1 mL) was lyophilized at –70 ℃ for 2 h, under the pressure of 70 Pa. After lyophilization, CQDs in solid state were added into soft tin containers and burned in the furnace at 950 ℃ of the CHNS elemental analyzer. Data obtained from the CHNS elemental analyzer showed that the CQDs sample contained 46 % of carbon and 7.1 % of hydrogen. Traces of nitrogen and sulfur were not found in the analyzed sample.

Interactions of ssDNA (10 μg mL^{-1}) and dsDNA (10 μg mL^{-1}) with CQDs were studied separately with different amounts of added CQDs. Samples of CQDs at the corresponding concentration were mixed with ssDNA and dsDNA solutions and the changes in the absorption spectra were monitored by spectrophotometry. The CQDs–DNA absorbance maximum was observed at 260 nm. It clearly follows from the results showed in Fig. 2A that increasing the concentration of CQDs mixed with DNA results in a gradual increase of the CQDs absorption. This can be caused by the interaction of the electron pairs of oxygen atoms from PEG with DNA bases forming hydrogen bonds. From the obtained results it can be concluded that the absorbance of CQDs increases with their increasing concentration. However, results of CQDs–ssDNA measurements showed that the absorbance gradually increases with the increasing concentration of CQDs, but no changes in the absorbance were observed in the concentration range of 50–100 μg mL^{-1}, followed by a gradual increase of the absorbance. In case of the CQDs–dsDNA sample, the absorbance gradually increased and then a slight decrease was observed at 50 μg mL^{-1}, from this point, the absorbance continued to increase gradually (Fig. 2A).

As previously mentioned, the interactions of ssDNA and dsDNA with CQDs were studied separately with different amounts of CQDs and the fluorescence was measured at the excitation wavelengths of 280 nm, 350 nm, and 400 nm for CQDs and DNA. When the excitation wavelength of 280 nm was used, a narrow peak at 376 nm was found. The fluorescence intensity at 376 nm increased due to the CQDs concentration increase, which can be seen from the obtained fluorescence intensity in Fig. 2B. From the results obtained, it can be seen that the fluorescence intensity of CQDs gradually increased with the increasing concentration of CQDs in the sample. However, the mixture of CQDs and ssDNA showed certain variation in the fluores-

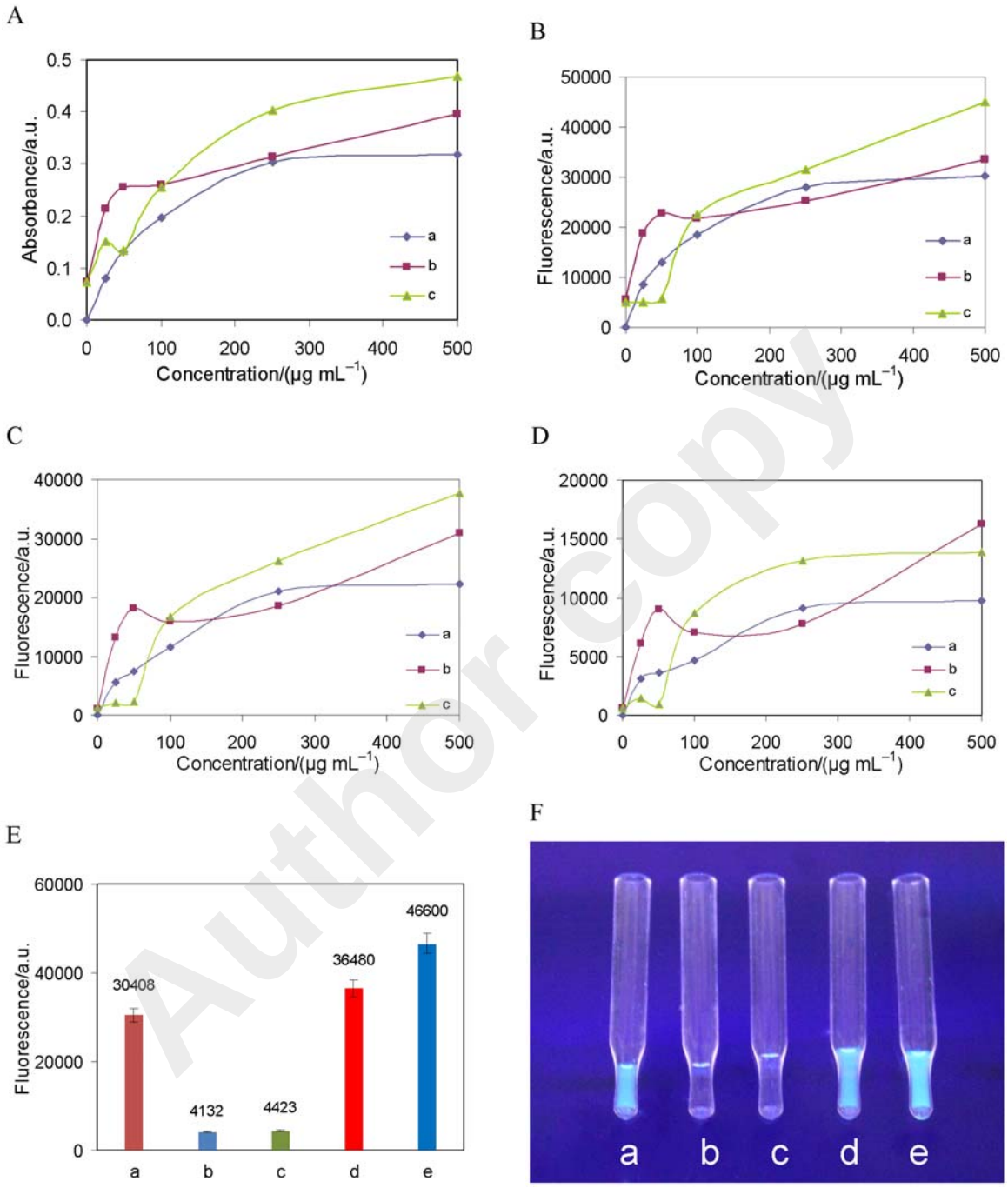

Fig. 2. Absorption and fluorescence spectra of CQDs–DNA (10 μg mL^{-1} of ssDNA or dsDNA) with different amounts of CQDs (μg mL^{-1}: 25, 50, 100, 250, and 500): influence of the increasing concentration of CQDs (a) CQDs–ssDNA (b), and CQDs–dsDNA (c) on the absorbance (A); influence of the increasing concentration of CQDs (a), CQDs–ssDNA (b), and CQDs–dsDNA (c) on the fluorescence measured at the excitation wavelengths of 280 nm (B), 350 nm (C), and 400 nm (D), respectively; fluorescence intensity of CQDs–DNA (F): CQDs (a), ssDNA (b), dsDNA (c), CQDs–ssDNA (d), CQDs–dsDNA (e); fluorescent image taken under the UV excitation at 312 nm (F): CQDs (a), ssDNA (b), dsDNA (c), CQDs–ssDNA (d), CQDs–dsDNA (e).

cence intensity. At lower concentrations, the fluorescence intensity of CQDs mixed with ssDNA rapidly increased but then it showed gradual decrease in the concentration range of 50–100 μg mL^{-1}, followed by further gradual increase of the fluorescence intensity at higher concentrations. The variation in the fluorescence intensity at 376 nm can be explained by the adsorption of ssDNA on the surface of CQDs via π–π interactions (Ding et al., 2014). In case of the CQDs–dsDNA sample, the variation of the fluorescence intensity is also noticeable; however, in contrast to the CQDs–ssDNA sample, it can be seen that the fluores-

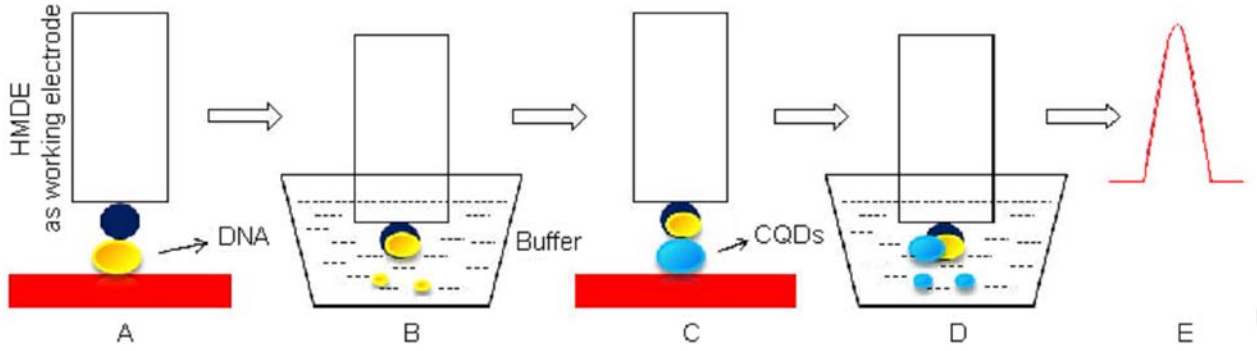

Fig. 3. Scheme of the adsorptive transfer technique for the interaction of DNA and CQDs: working electrode is immersed in a drop containing the target molecule (DNA) to be adsorbed on the surface of this electrode (A); DNA-modified HMDE is rinsed in the buffer (B); the electrode is transferred to the solution containing CQDs to allow their interaction with molecules adsorbed in the previous step (C); after another rinsing step (D), the adsorbed complex is detected in the presence of supporting electrolyte; adsorbed complex is consequently electrochemically analyzed (E).

cence intensity of CQDs/dsDNA gradually decreased in the concentration range of 25–50 μg mL^{-1}, and then it gradually increased at higher concentrations. From these results it can be concluded that CQDs are bound into the structure of dsDNA. In such a case it is assumed that electron pairs of oxygen atoms from PEG can be bound with DNA bases by hydrogen bonds, but according to Li et al. (2013b), four different mechanism can be adopted for QDs and DNA binding: QDs externally bind to DNA backbones while DNA wraps around QDs; QDs seemingly generate DNA loops by simultaneously binding to two different sites on a DNA molecule; QDs form a bridge to connect two or more DNA molecules together. This binding arises from the high affinity of QDs to DNA. It can be concluded that the tested ssDNA and dsDNA interact with CQDs.

For excitation wavelengths of 350 nm, the emission peak was found at 430 nm (Fig. 2C), while the measurement at 400 nm showed an emission peak at 464 nm (Fig. 2D). In these two cases, the fluorescence intensity was found to be much lower in comparison with that at the emission wavelength of 280 nm. Fluorescence intensity decreased in all samples when the excitation wavelength increased. However, ssDNA and dsDNA have very low fluorescence intensity whereas they showed high intensity when mixed with CQDs, in such a case, dsDNA showed higher intensity than ssDNA (Figs. 2E and 2F).

DNA–CQDs interaction

Square wave voltammetry coupled with the adsorptive transfer technique is one of the most sensitive methods for DNA detection (Bartošík & Paleček, 2011; Krejcova et al., 2013). The adsorptive transfer technique is based on the strong adsorption of the target molecule on the surface of the working electrode (Huska et al., 2009). In this study, interactions of dsDNA and ssDNA with CQDs on the surface of a working electrode were studied, which is shown in Fig. 3. A 5 μL sample of DNA (dsDNA or ssDNA) (concentration of 1 μg mL^{-1}) was placed on Parafilm. A hanging mercury drop electrode (HMDE) was subsequently immersed into this drop. DNA was accumulated for 120 s on the surface of the immersed HMDE. After the accumulation step, HMDE was rinsed. The DNA-modified HMDE was subsequently transferred into 5 μL of CQDs, and then rinsed and transferred into a supporting electrolyte after a certain time interval. The absorbed complex was consequently electrochemically analyzed (Paleček, 2002; Paleček & Fojta, 2001).

Electrochemical detection of CA peak from DNA–CQDs complexes

The ability of nucleic acids to produce analytically useful electrochemical reduction and oxidation signals was first reported by the end of the 1950s and at the beginning of the 1960s (Paleček, 1960, 1961). These signals originate from the residues of bases in DNA. Adenine (A) and cytosine (C) residues in DNA produce reduction signals. Guanine (G) produces a specific anodic signal explained by the oxidation of the DNA reduction product formed at highly negative potentials (Paleček, 2002). The main aim of this study is to monitor the changes of the cytosine adenine (CA) signal from complex of ssDNA and dsDNA with CQDs. Measurements were conducted separately for each DNA type with the prolonging interaction time and increasing CQDs concentration.

dsDNA–CQDs complex

CA peak of dsDNA was determined at (–1.42 ± 0.01) V (Fig. 4A). Accumulation time of dsDNA was optimized to 120 s. Interaction time (0 s, 30 s, 60 s, 90 s, and 120 s) of dsDNA and CQDs was determined.

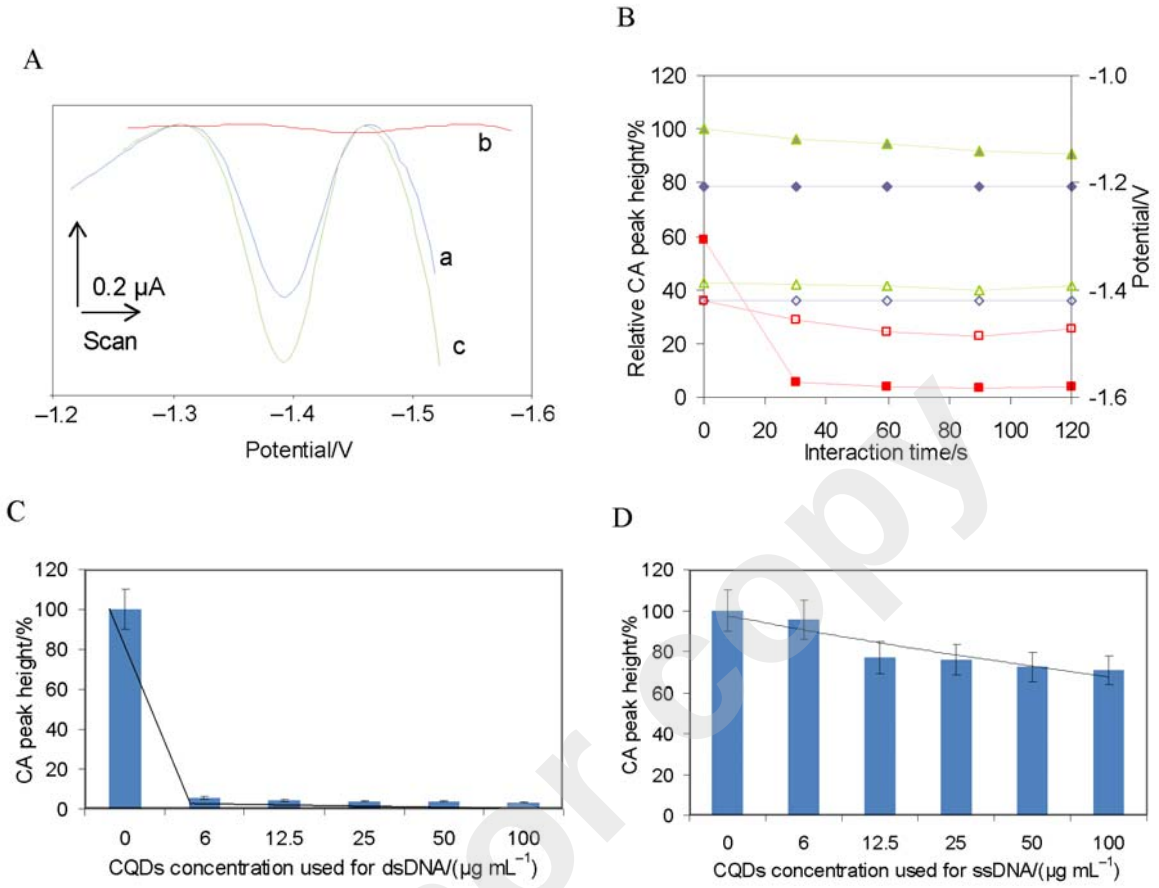

Fig. 4. Typical SW voltammograms of dsDNA (a), dsDNA–CQDs (b), and ssDNA–CQDs (c) complexes (A); dependence of relative CA peak height (solid circle, solid square and solid triangle) and potential (empty circle, empty square and empty triangle) on the interaction time of CQDs with DNA (B) as: dsDNA (a), dsDNA–CQDs complex (b), ssDNA–CQDs complex (c), dsDNA (d), dsDNA–CQDs complex (e), ssDNA–CQDs complex (f); dependence of relative CA peak height on the CQDs concentration used in their interaction with dsDNA (C) and with ssDNA (D). The AdT SWV method was used. Parameters of AdT SWV were as follows: time of accumulation: 120 s; time of interaction: 30 s (C), 120 s (D); purge time: 120 s; frequency: 280 Hz; initial potential: 0 V; end potential –1.8 V; step potential: 0.005 V; amplitude: 0.025 V.

Height of the CA peak of the dsDNA–CQDs complex decreased linearly until the interaction time of 120 s (Fig. 4B). Thus, the relative CA peak height of the dsDNA–CQDs complex was reduced by 20 % without the change of the of interaction time. It means that the interaction between dsDNA and CQDs occurs immediately. Furthermore, the relative CA peak height of the dsDNA–CQDs complex continuously decreased by more than 50 % after the interaction time of 30 s and then gradually decreased after the interaction time of 60 s, 90 s, and 120 s, respectively. The potential of the CA peak of dsDNA–CQDs significantly changed in comparison with that of the CA peak of dsDNA (Fig. 4A). The dependence of the concentration of CQDs on the interaction between dsDNA and CQDs was also studied (Fig. 4C). Different concentrations of CQDs were applied to study their interaction with dsDNA. The interaction time of 30 s was chosen as it provides the most rapidly decreasing signal. Accumulation time of dsDNA was 120 s. It can be seen that the signal of the CA peak of the dsDNA–CQDs complex diminishes linearly with the increase of the CQDs concentration, showing thus that the interaction of dsDNA with CQDs decreases the CA peak signal of dsDNA–CQDs depending on the increasing concentration of CQDs used in the dsDNA-CQDs interaction process. A hypothesis can be drawn that CQDs bind into the structure of dsDNA (Fig. 1). Moreover, the interaction between dsDNA and CQDs on the surface of the working electrode takes place immediately.

ssDNA–CQDs complex

For the detection of the CA peak of the ssDNA–CQDs complex, square wave voltammetry coupled with the adsorptive transfer technique was also employed. CA peak of ssDNA was determined at (–1.38 ± 0.01) V. The electrochemical signal of ssDNA is generally higher than that of dsDNA at the mercury and carbon electrodes (Bartošík & Paleček, 2011). This study provides the same results also for the HMDE. Interaction time (0 s, 30 s, 60 s, 90 s, and 120 s) of ssDNA and CQDs was studied, while the accumulation time of ssDNA was 120 s. The signal of the CA

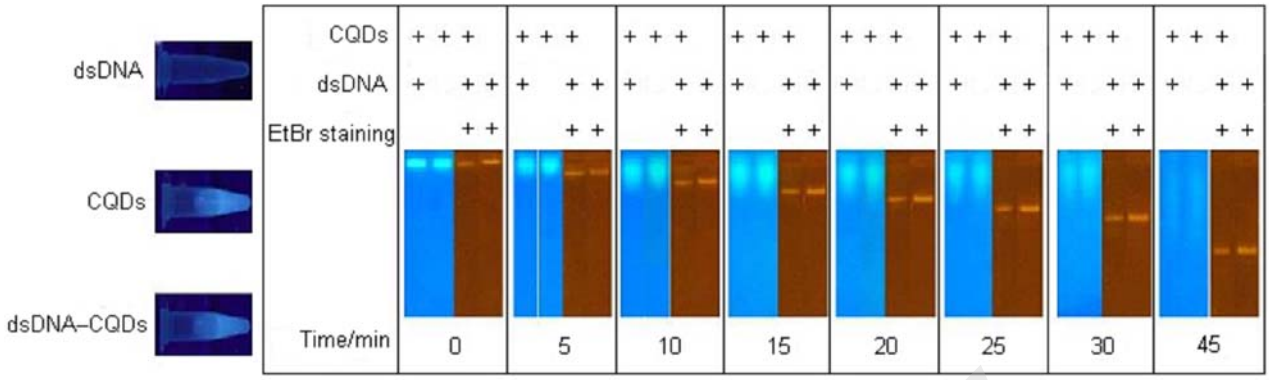

Fig. 5. Gel electrophoresis experiment using visualization by a UV transilluminator at 312 nm: Cutting part from gel of QDs with DNA without staining (first column); QDs without staining (second column); QDs with DNA after staining with ethidium bromide (third column); DNA after staining with ethidium bromide (fourth column).

peak of the ssDNA–CQDs complex decreased linearly until the interaction time of 120 s (Fig. 4B). Unlike the dsDNA–CQDs complex, the rate of the ssDNA–CQDs signal decrease was lower and the potential change was insignificant. The dependence of the concentration of CQDs on the interaction between ssDNA and CQDs was also observed (Fig. 4D). Different concentrations of CQDs were used in their interaction with ssDNA. The optimized accumulation time of ssDNA was 120 s. It can be seen that the signal of the CA peak of the ssDNA–CQDs complex decreases linearly with the increase of the CQDs concentration. The absorption of ssDNA on the surface of CQDs via π–π interactions resulted in the decrease of the CA peak signal depending on the increasing amount of CQDs in the ssDNA–CQDs interaction process.

Gel electrophoresis analysis of dsDNA

Using PEG-coated CQDs as a support for PCR amplification of dsDNA, substantial DNA coupled with CQDs was provided under optimized conditions. In this part of the experiment, 10 mL of CQDs were ten times concentrated to 1 mL using lyophilization at –70 ℃ for 2 h under the pressure of 70 Pa. For each sample, the DNA concentration was 300 μg mL^{-1}. The samples were diluted in the ratio of 1 : 1 to obtain the same concentration of DNA (150 μg mL^{-1}) and QDs in each. After the PCR reaction, the gel electrophoresis experiment was carried out to investigate the successful extension of CQDs–DNA conjugates (Fig. 5). The PCR product was mixed with CQDs and processed by the 2 % agarose gel electrophoresis for 0 min, 5 min, 10 min, 15 min, 20 min, 25 min, 30 min, and 45 min at 60 V, 400 mA and 25 ℃. The band of CQDs with a DNA strand (lane 1), CQDs (lane 2), CQDs with a DNA strand and ethidium bromide (lane 3), and a DNA strand with ethidium bromide (line 4) were observed by a UV transilluminator. From these lanes it can be seen that with the changing interaction time, migration time of the samples also change. Lane 1 corresponds to the injection of CQDs mixed with DNA in the gel.

It can be clearly seen from Fig. 5, that the smear area in lane 2 (CQDs) is slighty larger and brighter than that in lane 1 (CQDs–dsDNA), which suggests that CQDs were bound into the structure of dsDNA. To verify the hypothesis that the CQDs interact with DNA, the samples were stained with ethidium bromide, which serves as a fluorescent label for DNA visualization. On the lanes stained with ethidium bromide, the influence of CQDs concentration on DNA was determined. Lane 3 shows the sample of CQDs–DNA stained with ethidium bromide. As the DNA is distorted by the presence of CQDs, the labeling fluorescence intensity is reduced. In lane 4, only DNA was stained with ethidium bromide and from this lane, the high fluorescence intensity of DNA with the same migration time of sample as in other cases can be seen. A comparison of lanes 3 and 4 shows that the sample with DNA has higher fluorescence intensity than those with CQDs, which is probably caused by the CQDs being bound into the DNA strand blocking the ethidium bromide binding into the DNA structure. The intercalation of CQDs into the DNA structure also leads to changes in the electrophoretic behavior of the CQDs–DNA complexes (Wang et al., 2010b).

Conclusions

In summary, structurally and optically stable CQDs functionalized with DNA can be successfully produced. Investigation of the physicochemical interactions between CQDs and DNA during their conjugation, spectral methods, electrophoresis, and electrochemical analysis provide an insight into the major experimental parameters determining the CQDs functionalization with DNA. According to the obtained data, it can be assumed that the ssDNA strand conjugates with CQDs via π–π interactions. The interaction between CQDs and dsDNA indicates that CQDs are bound into the structure of dsDNA via electron

pairs of oxygen atoms from PEG bound with DNA bases by hydrogen bonds. PEG bounded into the ds-DNA significantly increases the fluorescence of CQDs. ssDNA can also increase the fluorescence of CQDs, but such an increase is lower than that of dsDNA due to the weaker bond between ssDNA and PEG. These CQDs–DNA conjugates are optically stable. However, this paper presents a potential application of CQDs in the design of highly sensitive biosensors.

Acknowledgements. Financial support from CEITEC CZ.1.05/1.1.00/02.0068 is highly acknowledged. The authors wish to thank Lukas Melichar for perfect technical assistance.

References

Bai, W. J., Zheng, H. Z., Long, Y. J., Mao, X. J., Gao, M., & Zhang, L. (2011). A carbon dots-based fluorescence turn-on method for DNA determination. *Analytical Sciences*, *27*, 243–246. DOI: 10.2116/analsci.27.243.

Bartošík, M., & Paleček, E. (2011). Square wave stripping voltammetry of unlabeled single- and double-stranded DNAs. *Electroanalysis*, *23*, 1311–1319. DOI: 10.1002/elan.201100079.

Bourlinos, A. B., Stassinopoulos, A., Anglos, D., Zboril, R., Karakassides, M., & Giannelis, E. P. (2008) Surface functionalized carbogenic quantum dots. *Small*, *4*, 455–458. DOI: 10.1002/smll.200700578.

Cao, L., Wang, X., Meziani, M. J., Lu, F., Wang, H., Luo, P. G., Lin, Y., Harruff, B. A., Veca, L. M., Murray, D., Xie, S. Y., & Sun, Y. P. (2007). Carbon dots for multiphoton bioimaging. *Journal of the American Chemical Society*, *129*, 11318–11319. DOI: 10.1021/ja073527l.

Ding, C., Zhu, A., & Tian, Y. (2014). Functional surface engineering of C-dots for fluorescent biosensing and in vivo bioimaging. *Accounts of Chemical Research*, *47*, 20–30. DOI: 10.1021/ar400023s.

Dong, Y., Zhou, N., Lin, X., Lin, J., Chi, Y., & Chen, G. (2010). Extraction of electrochemiluminescent oxidized cCarbon quantum dots from activated carbon. *Chemistry of Materials*, *22*, 5895–5899. DOI: 10.1021/cm1018844.

Dong, Y., Wang, R., Li, H., Shao, J., Chi, Y., Lin, X., & Chen, G. (2012a). Polyamine-functionalized carbon quantum dots for chemical sensing. *Carbon*, *50*, 2810–2815. DOI: 10.1016/j.carbon.2012.02.046.

Dong, Y., Wang, R., Li, G., Chen, C., Chi, Y., & Chen, G. (2012b). Polyamine-functionalized carbon quantum dots as fluorescent probes for selective and sensitive detection of copper ions. *Analytical Chemistry*, *84*, 6220–6224. DOI: 10.1021/ac3012126.

Dong, Y., Chen, C., Lin, J., Zhou, N., Chi, Y., & Chen, G. (2013). Electrochemiluminescence emission from carbon quantum dot-sulfite coreactant system. *Carbon*, *56*, 12–17. DOI: 10.1016/j.carbon.2012.12.086.

Fu, A., Gu, W., Larabell, C., & Alivisatos, A. P. (2005). Semiconductor nanocrystals for biological imaging. *Current Opinion in Neurobiology*, *15*, 568–575. DOI: 10.1016/j.conb.2005.08.004.

Grimes, A. F., Call, S. E., Vicente, D. A., English, D. S., & Harbron, E. J. (2006). Toward efficient photomodulation of conjugated polymer emission: Optimizing differential energy transfer in azobenzene-substituted PPV derivatives. *The Journal of Physical Chemistry B*, *110*, 19183–19190. DOI: 10.1021/jp0613236.

He, S., Huang, B. H., Tan, J., Luo, Q. Y., Lin, Y., Li, J., Hu, Y., Zhang, L., Yan, S., Zhang, Q., Pang, D. W., & Li, L. (2011). One-to-one quantum dot-labeled single long DNA probes. *Biomaterials*, *32*, 5471–5477. DOI: 10.1016/j.biomaterials.2011.04.013.

Huska, D., Fabrik, I., Baloun, J., Adam, V., Masarik, M., Hubalek, J., Vasku, A., Trnkova, L., Horna, A., Zeman, L., & Kizek, R. (2009). Study of interactions between metallothionein and cisplatin by using differential pulse voltammetry Brdicka's reaction and quartz crystal microbalance. *Sensors*, *9*, 1355–1369. DOI: 10.3390/s90301355.

Jia, X., Li, J., & Wang, E. (2012). One-pot green synthesis of optically pH-sensitive carbon dots with upconversion luminescence. *Nanoscale*, *4*, 5572–5575. DOI: 10.1039/c2nr31319g.

Kim, J., Park, J., Kim, H., Singha, K., & Kim, W. J. (2013). Transfection and intracellular trafficking properties of carbon dot-gold nanoparticle molecular assembly conjugated with PEI-pDNA. *Biomaterials*, *34*, 7168–7180. DOI: 10.1016/j.biomaterials.2013.05.072.

Krejcova, L., Hynek, D., Kopel, P., Rodrigo, M. A. M., Tmejova, K., Trnkova, L., Adam, V., Hubalek, J., & Kizek, R. (2013). Quantum dots for electrochemical labelling of neuramidinase genes of H5N1, H1N1 and H3N2 influenza. *International Journal of Electrochemical Science*, *8*, 4457–4471.

Kwon, W., Do, S., Won, D. C., & Rhee, S. W. (2013). Carbon quantum dot-based field-effect transistors and their ligand length-dependent carrier mobility. *ACS Applied Materials & Interfaces*, *5*, 822–827. DOI: 10.1021/am3023898.

Li, H., Ming, H., Liu, Y., Yu, H., He, X., Huang, H., Pan, K., Kang, Z., & Lee, S. T. (2011a). Fluorescent carbon nanoparticles: electrochemical synthesis and their pH sensitive photoluminescence properties. *New Journal of Chemistry*, *35*, 2666–2670. DOI: 10.1039/c1nj20575g.

Li, H., He, X., Liu, Y., Huang, H., Lian, S., Lee, S. T., & Kang, Z. (2011b). One-step ultrasonic synthesis of water-soluble carbon nanoparticles with excellent photoluminescent properties. *Carbon*, *49*, 605–609. DOI: 10.1016/j.carbon.2010.10.004.

Li, Y., Zhang, B. P., Zhao, J. X., Ge, Z. H., Zhao, X. K., & Zou, L. (2013a). ZnO/carbon quantum dots heterostructure with enhanced photocatalytic properties. *Applied Surface Science*, *279*, 367–373. DOI: 10.1016/j.apsusc.2013.04.114.

Li, K., Zhang, W., & Chen, Y. (2013b). Quantum dot binding to DNA: Single-molecule imaging with atomic force microscopy. *Biotechnology Journal*, *8*, 110–116. DOI: 10.1002/biot.201200155.

Liang, Q., Ma, W., Shi, Y., Li, Z., & Yang, X. (2013). Easy synthesis of highly fluorescent carbon quantum dots from gelatin and their luminescent properties and applications. *Carbon*, *60*, 421–428. DOI: 10.1016/j.carbon.2013.04.055.

Linehan, K., & Doyle, H. (2014). Efficient one-pot synthesis of highly monodisperse carbon quantum dots. *RSC Advances*, *4*, 18–21. DOI: 10.1039/c3ra45083j.

Liu, Y., Liu, C. Y., & Zhang, Z. Y. (2011). Synthesis and surface photochemistry of graphitized carbon quantum dots. *Journal of Colloid and Interface Science*, *356*, 416–421. DOI: 10.1016/j.jcis.2011.01.065.

Liu, S., Tian, J., Wang, L., Luo, Y., & Sun, X. (2012). A general strategy for the production of photoluminescent carbon nitride dots from organic amines and their application as novel peroxidase-like catalysts for colorimetric detection of H_2O_2 and glucose. *RSC Advances*, *2*, 411–413. DOI: 10.1039/c1ra00709b.

Long, Y. M., Zhou, C. H., Zhang, Z. L., Tian, Z. Q., Bao, L., Lin, Y., & Pang, D. W. (2012). Shifting and non-shifting fluorescence emitted by carbon nanodots. *Journal of Materials Chemistry*, *22*, 5917–5920. DOI: 10.1039/c2jm30639e.

Ming, H., Ma, Z., Liu, Y., Pan, K., Yu, H., Wang, F., & Kang, Z. (2012). Large scale electrochemical synthesis of high quality

carbon nanodots and their photocatalytic property. *Dalton Transactions*, *41*, 9526–9531. DOI: 10.1039/c2dt30985h.

Paleček, E. (1960). Oscillographic polarography of highly polymerized deoxyribonucleic acid. *Nature*, *188*, 656–657. DOI: 10.1038/188656a0.

Paleček, E. (1961). Oscillographic polarography of deoxyribonucleic acid degradation products. *Biochimica et Biophysica Acta*, *51*, 1–8. DOI: 10.1016/0006-3002(61)91010-1.

Paleček, E., & Fojta, M. (2001). Detecting DNA hybridization and damage. *Analytical Chemistry*, *73*, 74A–83A. DOI: 10.1021/ac0123936.

Paleček, E. (2002). Past, present and future of nucleic acids electrochemistry. *Talanta*, *56*, 809–819. DOI: 10.1016/s0039-9140(01)00649-x.

Pandey, A. P., Karande, K. P., More, M. P., Gattani, S. G., & Deshmukh, P. K. (2014). Graphene based nanomaterials: Diagnostic applications. *Journal of Biomedical Nanotechnology*, *10*, 179–204. DOI: 10.1166/jbn.2014.1773.

Pohanka, M. (2014). Biosensors containing acetylcholinesterase and butyrylcholinesterase as recognition tools for detection of various compounds. *Chemical Papers*, in press. DOI: 10.2478/s11696-014-0542-x.

Ryvolova, M., Chomoucka, J., Drbohlavova, J., Kopel, P., Babula, P., Hynek, D., Adam, V., Eckschlager, T., Hubalek, J., Stiborova, M., Kaiser, J., & Kizek, R. (2012). Modern micro and nanoparticle-based imaging techniques. *Sensors*, *12*, 14792–14820. DOI: 10.3390/s121114792.

Sahu, S., Behera, B., Maiti, T. K., & Mohapatra, S. (2012). Simple one-step synthesis of highly luminescent carbon dots from orange juice: application as excellent bio-imaging agents. *Chemical Communications*, *48*, 8835–8837. DOI: 10.1039/c2cc33796g.

Song, Y., Feng, D., Shi, W., Li, X., & Ma, H. (2013). Parallel comparative studies on the toxic effects of unmodified CdTe quantum dots, gold nanoparticles, and carbon nanodots on live cells well as green gram sprouts. *Talanta*, *116*, 237–244. DOI: 10.1016/j.talanta.2013.05.022.

Su, Y., Xie, Y., Hou, X., & Lv, Y. (2014). Recent advances in analytical applications of nanomaterials in liquid-phase chemiluminescence. *Applied Spectroscopy Reviews*, *49*, 201–232. DOI: 10.1080/05704928.2013.819514.

Vaishnavi, E., & Renganathan, R. (2014). "Turn-on-off-on" fluorescence switching of quantum dots–cationic porphyrin nanohybrid: a sensor for DNA. *Analyst*, *139*, 225–234. DOI: 10.1039/c3an01871g.

Wang, F., Pang, S., Wang, L., Li, Q., Kreiter, M., & Liu, C. Y. (2010a). One-step synthesis of highly luminescent carbon dots in noncoordinating solvents. *Chemistry of Materials*, *22*, 4528–4530. DOI: 10.1021/cm101350u.

Wang, C., Gao, X., & Su, X. (2010b). Study the damage of DNA molecules induced by three kinds of aqueous nanoparticles. *Talanta*, *80*, 1228–1233. DOI: 10.1016/j.talanta.2009.09.014.

Wang, J., Shan, Y., Zhao, W. W., Xu, J. J., & Chen, H. Y. (2011). Gold nanoparticle enhanced electrochemiluminescence of CdS thin films for ultrasensitive thrombin detection. *Analytical Chemistry*, *83*, 4004–4011. DOI: 10.1021/ac200616g.

Yang, T., Lu, M., Mao, X., Liu, W., Wan, L., Miao, S., & Xu, J. (2013). Synthesis of CdS quantum dots (QDs) via a hot-bubbling route and co-sensitized solar cells assembly. *Chemical Engineering Journal*, *225*, 776–783. DOI: 10.1016/j.cej.2013.04.028.

Zhang, X., Ming, H., Liu, R., Han, X., Kang, Z., Liu, Y., & Zhang, Y. (2013). Highly sensitive humidity sensing properties of carbon quantum dots films. *Materials Research Bulletin*, *48*, 790–794. DOI: 10.1016/j.materresbull.2012.11.056.

Zhao, D., Li, J., Yang, T., & He, Z. (2014). "Turn off–on" fluorescent sensor for platinum drugs-DNA interactions based on quantum dots. *Biosensors and Bioelectronics*, *52*, 29–35. DOI: 10.1016/j.bios.2013.08.031.